

## Multicritical point involving hexatic smectic phases

W. Pyżuk, E. Górecka, J. Szydłowska, A. Krówczyński,  
and D. Pociecha

*Laboratory of Dielectric and Magnetics, Department of Chemistry, Warsaw University, Al. Żwirki i Wigury 101,  
02-089 Warsaw, Poland*

J. Przedmojski

*Department of Physics, Warsaw Technical University, ul. Koszykowa 75, 00-662 Warsaw, Poland*

(Received 27 December 1994)

The triple point smectic-*C*–smectic-*F*–hexatic-*B* (*C-F-B*) has been found in binary mixtures of THI-*n* (thienyl-enaminoketone derivatives) compounds with different length of molecular terminal chains *n*. Differential scanning calorimetry (DSC), x-ray scattering, and optical studies show that this point is a multicritical point, where two continuous phase transition lines, Sm-*F*–Hex-*B* and Sm-*C*–Hex-*B*, meet. The topology of the phase diagram is different from that for the nematic–Sm-*A*–Sm-*C* (*N-A-C*) multicritical point. On the Sm-*F*–Hex-*B* line a tricritical point was observed for the system close to the Sm-*F*–Hex-*B*–Cry-*B* triple point. For mixtures of THI-*n* with some reference hexatic-*B* compounds, a phase diagram on which the Hex-*B*–Sm-*C* phase transition line extends between Sm-*C*–Sm-*F*–Hex-*B* and Sm-*A*–Sm-*C*–Hex-*B* multicritical points was found.

PACS number(s): 64.70.Md, 61.30.Eb

Over the last 20 years the triple points in liquid-crystalline systems have been extensively studied both theoretically [1–5] and experimentally [3,6–10]. In the vicinity of such a point, a phase transition may be strongly influenced by fluctuations arising from the presence of the third phase. For binary mixtures, coexistence of three phases on a *T-X* (temperature-concentration) phase diagram is possible at a multicritical point, at which the phases become thermodynamically identical. An interesting feature of multicritical points is the universality of generic phase diagrams, which is already well established for the nematic–smectic-*A*–smectic-*C* (*N-A-C*) point [3,6–8]. Besides *N-A-C* systems, which have been examined in detail [3,6–8], some corresponding systems with a chiral nematic and Sm-*C* phase [9,10], as well as the systems with twist grain boundary phases [11], have been studied. Recently, hexatic systems exhibiting long-range bond-orientational order of  $6n$ -fold symmetry have been considered [12,13]. Some triple points have been reported involving orthogonal hexatic-*B* (Hex-*B*), tilted to-the-side smectic-*F* (Sm-*F*), and tilted to-the-edge smectic-*I* (Sm-*I*) phases. The points Sm-*A*–Sm-*C*–Sm-*F* (*A-C-F*) and Sm-*A*–Hex-*B*–Sm-*I* (*A-B-I*) were identified as ordinary triple points with three first-order phase transition lines [14,15]. However, based on symmetry considerations, it is possible that Sm-*A*–Sm-*C*–Hex-*B* [2,3,16] and Sm-*A*–Hex-*B*–Sm-*I* (or Sm-*F*) [13] points may be multicritical, since continuity of all involved phase transitions is allowed.

Calorimetric and x-ray scattering methods are ideal tools for the study of multicritical points. Polarizing microscopy on the other hand is less useful for constructing phase diagrams in the vicinity of Sm-*A*–Hex-*B*–Sm-*I* (or Sm-*F*) triple point because textural changes accompanying transitions between orthogonal phases are difficult to

observe. In order to control our results by optical methods, we searched for more convenient systems with the Sm-*C*–Sm-*F*–Hex-*B* triple point, where the orthogonal phases are replaced by their tilted counterparts (and vice versa). In such systems, instead of the continuous Hex-*B*–Sm-*A* phase transition, a first-order transition between Sm-*F* and Sm-*C* phases appears. Nevertheless, a multicritical character of the triple point is still possible, if other phase transitions, Hex-*B*–Sm-*C* and Sm-*F*–Hex-*B*, remain continuous. In such cases the width of the biphasic area, which represents a first-order phase transition line on a *T-X* phase diagram, is vanishingly small on approaching a meeting point with two lines of continuous transitions. In this paper, we present a binary system with the Sm-*C*–Sm-*F*–Hex-*B* (*C-F-B*) triple point, and argue that it is, in fact, a multicritical point. Another system with potentially a multicritical Sm-*A*–Sm-*C*–Hex-*B* (*A-C-B*) point is also presented.

Systems to be studied were chosen from mixtures of THI-*n* (thienyl-enaminoketone derivatives) and MPR-*n* (pyridyl-enaminoketone derivatives) compounds [17], where *n* denotes the number of carbon atoms in a terminal alkyl chain. All compounds, synthesized in a routine way [18], were carefully purified by crystallization; their final purity was not less than 99.5 mol %, as checked by differential scanning calorimetry (DSC). In pure THI-*n* compounds, we observed an unusual phase sequence from the Hex-*B* to the Sm-*C* phase via an intervening tilted hexatic Sm-*F* phase (Fig. 1). The consequence of a vanishing Sm-*F* phase for higher homologues in binary mixtures of long ( $n > 15$ ) and short ( $n < 16$ ) homologues is the appearance of a *C-F-B* triple point. The THI-13+THI-17 system (Fig. 2) has been chosen because of the convenient temperature and concentration range of the Sm-*F* phase. In mixtures, the location of a triple

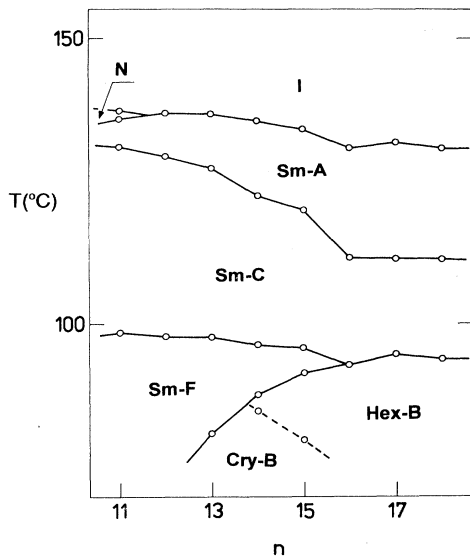


FIG. 1. Phase diagram,  $T$  vs  $n$ , for long chain THI- $n$  compounds. The Cry- $B$ -Hex- $B$  phase transition line is obtained from extrapolation of data for some binary systems [21].

point is defined by the mean terminal chain length (here  $n = 13 + 4X$ ,  $X$  is the molar fraction of THI-17) or, equivalently, by the number density of mesogenic cores. Since density is pressure dependent, a triple point should also be observed for THI-16 and higher homologues on  $T$ - $p$  phase diagrams of one-component systems. The phase sequence Hex- $B$ -Sm- $F$ -Sm- $C$  for shorter homologues provides an opportunity to generate another triple point, Sm- $A$ -Sm- $C$ -Hex- $B$ , in mixtures of THI- $n$  with compounds devoid of the Sm- $C$  phase, but having both the Hex- $B$  and Sm- $A$  orthogonal phases. We observed this point in several binary systems, e.g., in THI-14-MPR-6 mixtures (Fig. 3).

Phase diagrams were determined using both polarizing

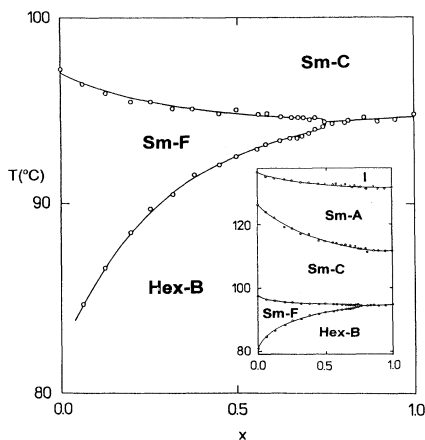


FIG. 2. Part of THI-13-THI-17 binary phase diagram with phase transition lines converging at  $C$ - $F$ - $B$  triple point. (In the inset, full phase diagram.) Lines are calculated according to Eq. (1). See the text for details.

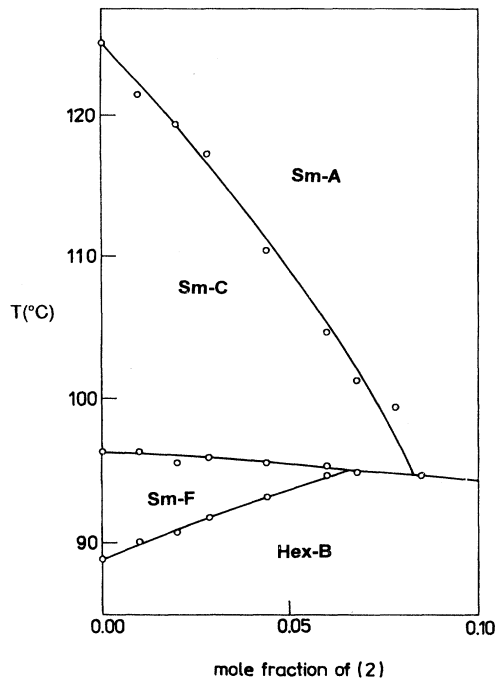


FIG. 3. Part of the phase diagram of THI-14 (component 1) with reference compound MPR-6 (component 2). Note two triple points,  $C$ - $F$ - $B$  and  $A$ - $C$ - $B$ , both possibly multicritical.

microscopy (Jenapol-Zeiss microscope equipped with Mettler FP82HT hot stage) and high-sensitive differential scanning calorimetry (Perkin-Elmer DSC-7). The latter method ensures greater precision in determination of phase transition temperatures for the hexatic phases. DSC thermograms were taken for several scanning rates covering one decade of magnitude, from 5 to 0.2°C/min, in order to extrapolate results to zero scan. Phase transition temperatures, determined with an accuracy of 0.01 K, coincided within 0.05°C when normalized to a given rate. In contrast, the thermal effects varied more or less with the scanning rate depending on the relations between phase transition enthalpy and contributions from pretransitional specific heat changes.

The x-ray experiments were performed in a reflection mode, using a modified spectrometer (DRON). For surface-free samples aligned on a surface treated cover glass, the wave vector was determined with the precision of  $1.10^{-3} \text{ \AA}^{-1}$ . Tilt angle was calculated as  $\theta = \cos^{-1}(d/d_B)$ , from layer spacing  $d$ , and reference spacing  $d_B$  for the smectic- $B$  phase. A conventional procedure referred to the smectic- $A$  phase has failed because of its high mean  $\theta$  angle ( $10^\circ$ - $15^\circ$ ).

The significant features of the phase transitions are as follows.

(i) The Hex- $B$ -Sm- $F$  phase transition far from the triple point is first order, as it is, e.g., for THI-14. Although this transition is tilt driven, a corresponding discontinuity in layer spacing was hardly detectable; the tilt change of  $3^\circ \pm 1^\circ$ , surprisingly small for this type of phase transition, is marked by the sharp peaks on the thermograms (Fig. 4) as well as by the invariant transition enthalpy,

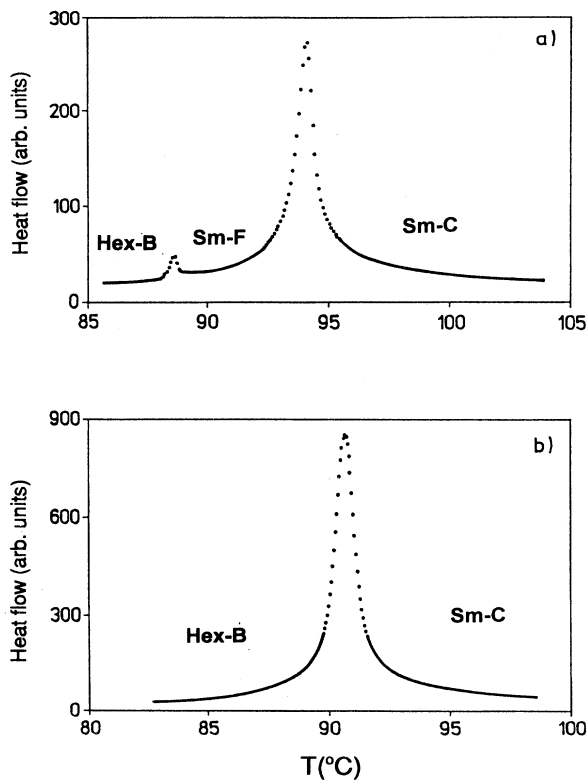


FIG. 4. Comparison of thermograms for Sm-*F*–Sm-*C* and Hex-*B*–Sm-*C* phase transitions in THI-13–THI-17 mixtures. THI-17 mol fractions are  $X=0.256$  (a) and  $0.802$  (b). Vertical scale, heat flow in arbitrary units.

$0.10 \pm 0.01 \text{ J g}^{-1}$ , with decreasing scanning rate. In contrast, for THI-15 and for the THI-13+THI-17 mixtures of concentrations from ca. 0.5 to 0.72 mole fraction of THI-17, close to the triple point, no abrupt tilt changes are observed (Fig. 5). On thermograms, there appear steps instead of peaks, which suggest a continuous phase transition with a small change, ca.  $0.1 \text{ J g}^{-1} \text{ K}^{-1}$ , in the specific heat. The different behavior of subsequent THI- $n$  homologues,  $n=14$  and  $15$ , is well confirmed by texture observations. It may be concluded, therefore, that the order of the phase transition between orthogonal and tilted hexatic phases is changed as the system moves away from the triple point. The appearance of a tricritical point on the Hex-*B*–Sm-*F* phase transition line can be attributed to the proximity of the crystalline Cry-*B* phase (cf. Fig. 1), which enhances crystalline order fluctuations within the Hex-*B* phase.

(ii) Both Sm-*F*–Sm-*C* and Hex-*B*–Sm-*C* phase transitions reveal similar DSC signal (Fig. 4) with pronounced  $c_p$  wings on both sides of the transition temperature. This reflects changes of both the in-plane density [13] and of the layer spacing. The presence of strong pretransitional anomalies makes any differentiation by DSC method between continuous and weakly discontinuous phase transitions impossible.

Only first-order transitions are allowed between tilted hexatic and smectic-*C* phases as a consequence of the same symmetry of both phases, thus tilt-induced hexatic-

ty of the *C* phase [3,19]. An alternative supercritical state evolution with no thermodynamic Sm-*F*–Sm- and Hex-*B*–Sm-*C* phase transition, which seems to correspond to smooth variation of the layer thickness (Fig. 6) as well as to the strong  $c_p$  anomalies (Fig. 4), should be excluded from further considerations. In case of continuity of Sm-*F* and Sm-*C* states, only the Hex-*B*–Sm-*F* and Hex-*B*–Sm-*C* phase transition line would remain on the phase diagram. A kink of this line (instead of the meeting point of three phase transition lines) is impossible in a homogeneous system for thermodynamic reasons. In conclusion, in the THI-13–THI-17 system, the Sm-*F*–Sm-*C* phase transition is first order, but due to the proximity of the critical end point, the relevant  $d$  discontinuities are too small to be observed in our experiment.

(iii) No jump in layer spacing has been observed for the Sm-*C*–Hex-*B* phase transition neither in mixtures, nor in pure THI-16. Thus, this transition may be continuous. Most surprising are the strong anomalies in layer spacing

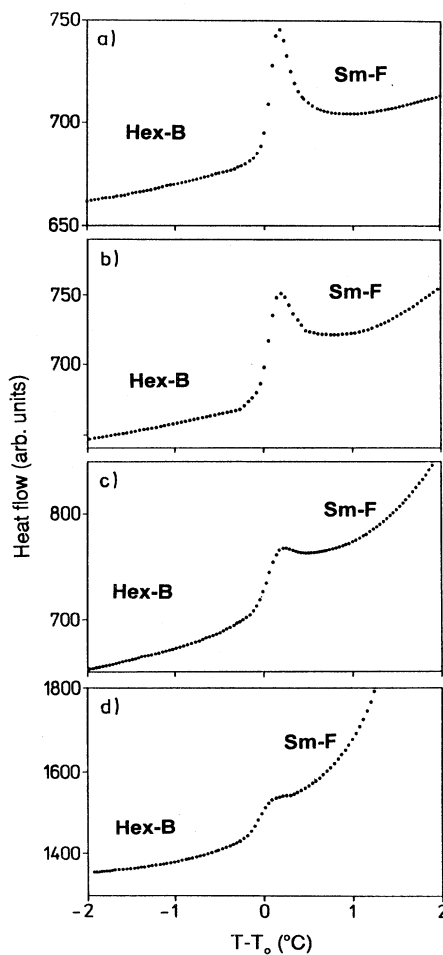


FIG. 5. Evolution of DSC thermograms, taken at  $2^\circ\text{C}/\text{min}$  scanning rate, along the Hex-*B*–Sm-*F* phase transition line in THI-13–THI-17 mixtures. THI-17 mol fractions are  $X=0.320$  (a)  $0.379$  (b)  $0.450$  (c), and  $0.621$  (d). Vertical scale; heat flow in arbitrary units; horizontal scale; distance from the phase transition.

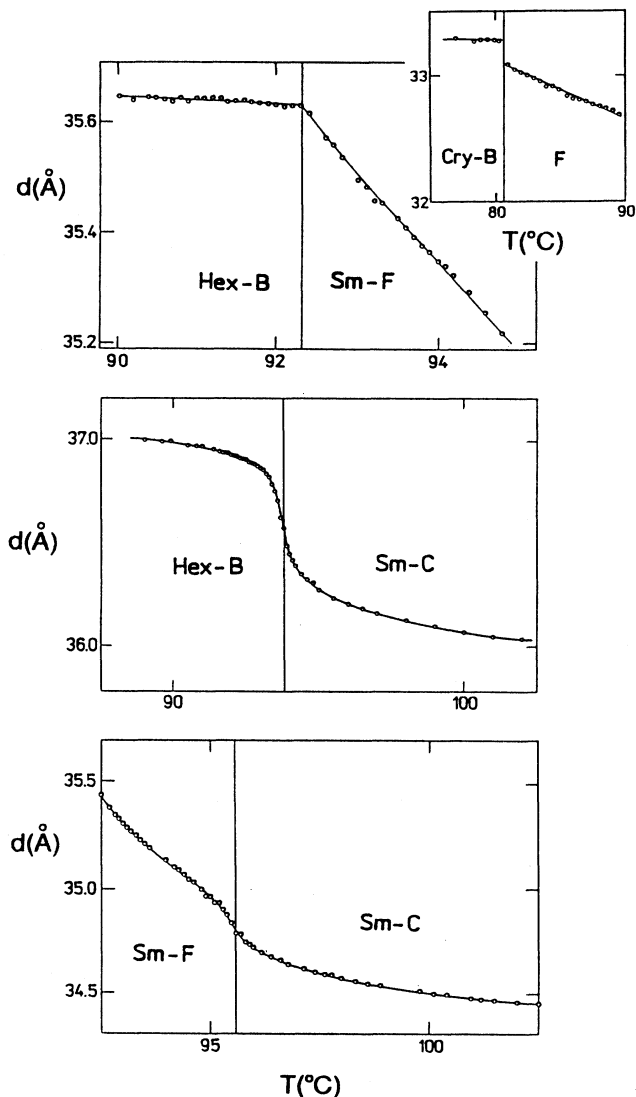


FIG. 6. Layer thickness for THI-*n* compounds in vicinity of phase transitions between hexatic phases, Hex-*B*–Sm-*F* (THI-15), and between hexatic and Sm-*C* phases, Hex-*B*–Sm-*C* (THI-16), and Sm-*F*–Sm-*C* (THI-15). In the inset, vicinity of Cry-*B*–Sm-*F* phase transition is shown for THI-13.

(Fig. 6) observed on both sides of this phase transition. The precritical layer anomalies in the Hex-*B* phase might suggest the appearance of induced tilt in the Hex-*B* phase. This behavior will be the subject of further studies.

For the case of converging two lines of continuous phase transitions the *C-F-B* point is a multicritical point, which is not in the same universality class as the *N-A-C* Lifshitz point [6,7]. This difference is shown by the topology of the relevant phase diagrams; for our system the smectic-*F* phase boundary seems to be parabolic near the *C-F-B* point, whereas no phase with such a property exists in *N-A-C* systems. The singular slope of the phase

transition lines at the apex makes the *C-F-B* systems particularly interesting for studies of fluctuations. For phase transition lines expressed as

$$T_{\alpha} = T_{BCF} + A_{\alpha} p^{\eta_{\alpha}} f_{\alpha}(p) + Bp, \quad (1)$$

where  $p = X_{BCF} - X$  is the distance from the triple point expressed in mole fraction of THI-17 and  $f(p)$  is a correcting function to a critical behavior. The topology is determined by the signs of amplitude  $A_{\alpha}$  and critical exponent  $\eta_{\alpha} - 1$  for all lines,  $\alpha = FC, BF, BC$  denotes Sm-*F*–Sm-*C*, Hex-*B*–Sm-*F*, and Hex-*B*–Sm-*C* phase transition lines, respectively.

So far, the shape of the order-disorder phase transition line has been calculated in an exactly solvable spherical model of a magnetic multicritical point of the Lifshitz type [20]. For an arbitrary dimensionality, critical exponents are  $\eta_h = \eta_f = d - 2.5$  (with the only exception of noncritical  $T_h$  behavior for  $d = 3$ ) and amplitude ratio  $A_h / A_f = 2^{1/2} \cos(\pi d / 2)$ . It is well known that the dimensionality enters crucially into liquid-crystalline properties. Although the relevance to the magnetic model still remains unexplained, the *N-A-C* systems are surprisingly well described by  $d = 3.075$  [6]. In these terms, our *C-F-B* system seems to correspond to an exact three-dimensional (3D) case, since no anomalous behavior of the Hex-*B*–Sm-*C* phase transition line is observed. The relevant exponent is  $\eta_{FC} = 0.5$ . Taking, by analogy to *N-A-C* systems [21],  $\eta_{FC} = \eta_{BF}$  we fitted the width of the *F* phase,  $T_{FC} - T_{BF}$ , and its boundaries. To recover the line shape in a wide concentration range, the correcting function  $f_{\alpha}(p) = \exp(C_{\alpha} p^{\delta_{\alpha}})$  was introduced into Eq. (1) and noncritical corrections,  $\delta_{\alpha} = 1$ , were sufficient to obtain a satisfactorily good fit. Unfortunately, no comparison to the expected phase diagrams could be made, since the phase coexistence in *C-F-B* systems has not been envisaged by theory so far.

In conclusion, we suggest a Sm-*C*–Sm-*F*–Hex-*B* triple point to be a new multicritical point, in which two hexatically ordered phases of different symmetries, Hex-*B* and Sm-*F*, coexist with a paraxial Sm-*C* phase. Another reported triple point, Sm-*A*–Sm-*C*–Hex-*B*, might also be multicritical, because it results from the convergence of two continuous phase transition lines involving the smectic-*C* phase. The third Hex-*B*–Sm-*A* phase transition should be continuous for systems sufficiently far from the Cry-*B*–Hex-*B*–*A* triple point [5]. We believe that this is the case for the THI-14+MPR-6 system, because the triple point is unattainable there [21] in spite of a wide concentration range. Among alternative topologies, the critical end point Sm-*A*–Sm-*C*–Hex-*B* has been predicted very recently [22].

The authors would like to thank Dr. Ray Folks for a critical reading of the manuscript and valuable comments. This work is a part of KBN Research Project No. 2P30302407. Chemical syntheses were supported by UW Grant No. 501-BST-472/94/95.

- [1] J. Chen and T. C. Lubensky, *Phys. Rev. A* **14**, 1202 (1976).
- [2] D. Johnson, D. Allender, R. de Hoff, C. Maze, E. Oppenheim, and R. Reynolds, *Phys. Rev. B* **16**, 470 (1977).
- [3] R. Bruinsma and D. Nelson, *Phys. Rev. B* **23**, 402 (1981).
- [4] D. L. Johnson, *J. Chim. Phys.* **80**, 45 (1983).
- [5] A. Aharony, R. J. Birgenau, J. D. Brock, and J. D. Litster, *Phys. Rev. Lett.* **57**, 1012 (1986).
- [6] D. Brisbin, D. L. Johnson, H. Fellner, and M. E. Neubert, *Phys. Rev. Lett.* **50**, 178 (1983).
- [7] R. Shadhidar, B. R. Ratna, and S. Krishna Prasad, *Phys. Rev. Lett.* **53**, 2141 (1984).
- [8] L. J. Martinez-Miranda, A. R. Kortan, and R. J. Birgenau, *Phys. Rev. Lett.* **56**, 2264 (1986); *Phys. Rev. A* **36**, 2372 (1987).
- [9] S. C. Parmar, N. A. Clark, D. M. Walba, and M. D. Ward, *Phys. Rev. Lett.* **62**, 2136 (1989).
- [10] J. Zubiz, M. Castro, J. A. Puertolas, J. Extebarria, M. A. Perez Jubindo, and M. P. de la Fuentes, *Phys. Rev. E* **48**, 1970 (1993).
- [11] S. R. Renn and T. C. Lubensky, *Mol. Cryst. Liq. Cryst.* **209**, 349 (1991).
- [12] J. D. Brock, R. J. Birgenau, J. D. Litster, and A. Aharony, *Contemp. Phys.* **30**, 321 (1989).
- [13] C. C. Huang and T. Stoebe, *Adv. Phys.* **42**, 3433 (1993).
- [14] V. N. Raja, D. S. Shankar Rao, and S. Krishna Prasad, *Phys. Rev. A* **46**, R726 (1992).
- [15] T. Pitchford, G. Nounesis, S. Dumrongrattana, J. Viener, C. C. Huang, and J. W. Goodby, *Phys. Rev. A* **32**, 1938 (1985).
- [16] Geetha G. Nair, V. N. Raja, S. Krishna Prasad, S. Chandrasekhar, and B. K. Sadashiva, in *Proceedings of the XIII AIRAPT International Conference on High Pressure Science and Technology*, edited by A. K. Singh (IBH, Oxford, 1991).
- [17] THI-*n* stands for 1-(4-alkoxyphenylamino)-3-[5''-(2''-methyl-thienyl)]-1-propen-3-one, MPR-*n* stands for 1-(4'-alkoxyphenylamino)-[3-(3''-pyridyl)]-1-propen-3-one, *n* denotes number of carbon atoms in alkoxy chain.
- [18] W. Pyżuk, A. Krówczyński, and E. Górecka, *Mol. Cryst. Liq. Cryst.* **237**, 75 (1993).
- [19] R. M. Hornreich, M. Luban, and S. Shtrikman, *Physica A* **86**, 463 (1977).
- [20] M. A. Anisimov and V. P. Voronov, *Mol. Cryst. Liq. Cryst.* **162A**, 1 (1988).
- [21] W. Pyżuk, J. Szydłowska, E. Górecka, A. Krówczyński, D. Pocięcha, and J. Przedmojski (unpublished).
- [22] A. D. Defontaine and J. Prost, *Phys. Rev. E* **47**, 1184 (1993).